ES Food and Agroforestry

DOI: https://dx.doi.org/10.30919/faf1953

Biosynthesis of Silver Nanoparticles Using *Raphanus sativus* Ethanolic Leaf Extract and Their Photocatalytic Degradation of Dyes from Polluted Water and Biological Activities

Sangeeta Gupta,[1] Amanpreet Kaur,[1,*] Man Vir Singh,[2,*] Deepanshu Rana,[3] Keshari Nandan,[4] Yogendra Kumar,[5] Shubham Sharma,[5] Avnish Chauhan[6] and Santosh Kumar Verma[7]

Abstract

This study explores the green synthesis of silver nanoparticles using *Raphanus sativus* leaf extracts, focusing on the identification of bioactive compounds responsible for nanoparticle stabilization and their characterization using a range of analytical techniques. Ultraviolet–Visible (UV-Vis) spectroscopy confirmed the successful synthesis of Rs-AgNPs, characterized by a distinct absorption peak at 435.009 nm. Fourier-transform infrared (FT-IR) spectroscopy revealed absorption bands indicative of phytoconstituents acting as capping agents. SEM investigation indicated that the dimensions of the Rs-AgNPs varied between 30 and 50 nm, while X-ray diffraction (XRD) analysis determined an average crystalline size of 21.85 nm. The photocatalytic efficiency of Rs-AgNPs was evaluated by the breakdown of methylene blue (MB) during UV light exposure. The DPPH and ABTS radical scavenging assays were used to assess antioxidant activity, yielding IC_{50} values of 18.41 and 25.78 µg/mL, respectively. Marked inhibitory effects were seen when evaluating antibacterial efficacy against Gram-positive (Listeria monocytogenes and Staphylococcus aureus) and Gram-negative (Escherichia coli and Pseudomonas aeruginosa) bacteria. An effective dosage-dependent inhibitory effect with significant zones of inhibition was observed for all examined bacterial strains. Furthermore, the inhibition experiments for α-amylase and α-glucosidase demonstrated encouraging antidiabetic effects, yielding IC_{50} values of 180.34 and 150.58 µg/mL, respectively. Silver nanoparticles synthesized from *Raphanus sativus* leaf extract exhibit antioxidant, antibacterial, and antidiabetic activities, indicating their potential in managing oxidative stress, combating bacterial infections, and supporting diabetes treatment.

Keywords: Raphanus sativus; Green AgNPs; Antioxidant; Antidiabetic; Photocatalysts.
Received: 18 March 2025; Revised: 01 December 2025; Accepted: 15 December 2025
Article type: Research article.

1. Introduction

Nanotechnology is an emerging and rapidly advancing discipline that has gained global attention due to the unique physicochemical and biological properties exhibited by nanomaterials.[1] This field enables the fabrication of novel materials with precise control over size, shape, and surface characteristics at the nanoscale. Nanoparticles play a vital role in diverse sectors, particularly in healthcare, energy production, and energy storage.[2] Metal nanoparticles can be synthesised using various approaches, including chemical, physical, eco-friendly (green), and hybrid methods. Among these, plant-based synthesis offers a sustainable and environmentally benign platform, as plants are biodegradable, biocompatible, and capable of producing nanoparticles in a cost-effective and eco-friendly manner.[3] Green synthesis typically utilises biological resources such as whole plants, fruits, roots, callus cultures, and other plant-derived materials. Fruit and vegetable wastes, although often discarded, possess substantial potential due to their abundance of vitamins and bioactive constituents. Peels from fruits and vegetables are particularly rich in nutrients such as vitamins, minerals, phenolic compounds, dietary fibre, and antioxidants.[4] For instance, apple peels contain high levels of vitamins A, K, and

[1]*Department of Chemistry, School of Sciences, IFTM University, Moradabad, Uttar Pradesh, 244102, India*
[2]*School of Applied and Life Sciences, UIT, Uttaranchal University, Dehradun, Uttarakhand, 248007, India*
[3]*Department of Microbiology, School of Lifesciences, Sardar Bhagwan Singh University, Dehradun, Uttar Pradesh, 248161, India*

C, along with significant amounts of calcium, potassium, and phenolic compounds, highlighting their value as a resource for nanoparticle synthesis.[5]

Metallic and metal oxide nanoparticles, especially silver nanoparticles (AgNPs), are widely employed across various fields, including agriculture, catalysis, bio-labelling, and biomedical sciences.[6] AgNPs are highly regarded for their potent antimicrobial properties,[4] which make them suitable for applications in food packaging, household products, and medical devices. In addition to antimicrobial activity, they exhibit antiplatelet, anticancer, and antioxidative properties.[7] Green synthesis using vegetable waste has emerged as an innovative and sustainable method for AgNP production, as it utilises readily available waste materials, reduces manufacturing costs, and avoids the use of hazardous chemicals.[8] Previous studies have employed waste materials such as potato peels and coriander stems to synthesise AgNPs, with investigations focusing on their cytotoxic, antibacterial, anticancer, and antioxidant activities.[9] Comparative analyses have also been conducted on the levels of secondary metabolites such as flavonoids, alkaloids, and phenolics in crude extracts versus AgNP formulations. Furthermore, enzyme inhibition assays, including protein kinase and α-amylase inhibition, have been used to evaluate the potential therapeutic efficacy of biosynthesised AgNPs.[10]

Recent research has increasingly emphasised the biosynthesis and characterisation of silver nanoparticles derived from vegetable waste, highlighting their relevance to green chemistry and sustainable nanotechnology. Green-synthesised AgNPs are not only environmentally favourable but also commercially viable, with the added benefit of being free from toxic chemical residues.[11] Plant extracts contribute to the stabilisation and reduction processes during nanoparticle formation owing to their intrinsic antioxidant and antimicrobial constituents. Kitchen waste has emerged as a valuable source of bioactive compounds for nanoparticle synthesis, as fruit and vegetable peels often contain up to 15% higher concentrations of phenolic compounds than the edible pulp.[12] This approach enhances waste utilisation, improves process efficiency, and supports sustainable waste management strategies. Biosynthesised AgNPs have demonstrated significant antibacterial activity, indicating their potential for applications such as the preservation of fruits and vegetables.[13,14] The present study focuses on the biosynthesis and characterisation of silver nanoparticles using ethanolic leaf extract of *Raphanus sativus*. Additionally, the biological properties and photocatalytic dye degradation potential of the synthesised AgNPs were evaluated to explore their suitability for environmental and biomedical applications.

[4]*Department of Chemistry, Gurukul Kangri Vishwavidyalaya, Haridwar, Uttar Pradesh, 249404, India*
[5]*Department of Chemistry, Institute of Applied Science & Humanities, GLA University, Mathura, Uttar Pradesh, 281406, India*
[6]*Department of Environmental Science, Graphic Era Hill University, Dehradun, Uttarakhand, 248002, India*
[7]*Chemistry and Chemical Engineering, Yulin University, Yulin 719000, China*
[*]*Email:* amanpreet2225@gmail.com (A. Kaur); manvir24365@gmail.com (M. V. Singh)

2. Materials and methods

2.1 Materials

Silver nitrate ($AgNO_3$), Muller Hilton Agar, 3-(4,5-dimethylthiazol-2-yl)-2,5-diphenyltetrazolium bromide (MTT), 2,2-diphenyl-1-picrylhydrazyl (DPPH), 2,2′-azinobis(3-ethylbenzothiazoline-6-sulfonic acid) (ABTS), and dimethyl sulfoxide (DMSO) were obtained from HiMedia. All supplementary compounds utilized were of analytical grade and obtained from reputable suppliers.

2.2 Extraction of Plant Material

2.2.1 Collection of plant material and preparation of extract

Raphanus sativus leaves were collected from Gumkhal, Pauri Garhwal, Uttarakhand, and taxonomically identified and verified by the Department of Botany, School of Sciences, IFTM University. A voucher specimen was deposited at this institution. The leaves were thoroughly washed with distilled water and then air-dried in the shade at ambient temperature. After drying, they were mixed into a powder using an electric laboratory blender.[15]

2.2.2 Extraction

A 100-gram sample was extracted with 600 milliliters of 99% ethanol using a Soxhlet apparatus for twenty hours. Subsequently, a rotary evaporator was used to concentrate filtered plant extract, then vacuum-dried to eliminate any residual solvents.[16] The % extract yield was determined using the following formula.

Yield% = Weight of extract/ weight of dried plant material×100

2.2.3 Phytochemical analysis

A preliminary phytochemical screening was conducted to identify the components found in the extracts of *Raphanus sativus*. The methodologies outlined by Shukla et al. (2020) were employed to identify the compounds, such as phenols, triterpenoids, tannins, flavonoids, saponins, and alkaloids.[17]

2.2.4 Green Synthesis of Silver Nanoparticles

The synthesis of AgNPs was facilitated by the ethanol extract of *Raphanus sativus* leaves, serving as a natural reducing and stabilising agent. For optimal reducing strength, a 1 mM aqueous solution of silver nitrate ($AgNO_3$) was used and mixed with a predetermined volume (1%, 2.5%, and 5% v/v) of the ethanol leaf extract. The findings were obtained at several temperatures (room temperature, 40 °C, 60 °C, and 80 °C) to assess the impact of temperature on nanoparticle production. The creation of nanoparticles was visibly

confirmed by the colour shift from light yellow to brown, indicating nanoparticle generation via surface plasmon resonance. Reactivities were maintained between 10 and 120 minutes to optimise the synthesis rate, while the pH of the solution was adjusted between 4 and 10 to assess its impact on nanoparticle production and stability. The optimal conditions for synthesis were determined to be a 5% extract concentration, a temperature of 60 °C, and a reaction period of 30 minutes, resulting in a neutral to slightly alkaline pH. Semidiurnal centrifugation facilitated the integration of the produced nanoparticles, which were further purified using distilled water and ethanol before being dried for further examination.

2.3 Characterization of AgNPs

UV−VIS Spectroscopic Measurements: The reduction of $AgNO_3$ was investigated using *Raphanus sativus* leaf extract by analysing the ultraviolet-visible spectrum. An HMG Labtech SPECTROstar Nano spectrophotometer was used to do this work. This apparatus was designed to function within the wavelength range of 220−700 nm, with a resolution of 1 nm.

FT-IR Measurements: The KBr pellet method and a PerkinElmer FT-IR spectrophotometer were used to examine the functional groups in the plant constituents accountable for the reduction and stabilisation of Rs-AgNPs. The spectra were recorded with a spectral resolution of 1 cm^{-1} throughout the range of 4000–400 cm^{-1}. XRD Analysis: The morphology and crystallinity of the biologically synthesised Rs-AgNPs were analysed using Powder X-ray diffraction (PXRD). Performance of measurements was implemented using a PANalytical Xpert PRO X-ray diffractometer, employing Cu Kα radiation (wavelength: 1.540 Å), and functioning at 45 kV and 30 mA. The scan was conducted at a rate of 0.02° within the 2θ range of 30° to 90°. FESEM The examination of surface shape, particle size, and elemental composition of metals in the biosynthesized Rs-AgNPs was performed using Field Emission Scanning Electron Microscopy (FESEM) with Energy Dispersive X-ray Spectroscopy (EDX). Morphology of the surface was analysed by ZEISS EVO scanning electron microscope at a magnification of 10,000×. The samples were attached to aluminium stubs using double-sided adhesive tape and later coated with a small coating of gold to enhance conductivity. The gold-coated samples were then examined microscopically to assess their morphology.

2.4 Antioxidant Activity

DPPH free radical scavenging method: The antioxidant potential of Rs-AgNPs was assessed by applying the DPPH radical scavenging technique. For the test, 100 µL of different doses of Rs-AgNPs and a standard (ascorbic acid) at 10 to 100 µg/mL were combined with 100 µL of DPPH solution (0.1 mM in 80% ethanol). The reaction mixture was incubated in the dark at 37 °C for 35 half an hour. The Systronic UV-1800 spectrophotometer was employed to measure absorbance at 517 nm, with ethanol serving as the blank solution. The proportion of DPPH radical scavenging activity was calculated using the given formula.[18]

$$\%\ of\ Inhibition = \frac{Absorbance\ of\ control\ -\ (absorbance\ of\ extract)}{Absorbance\ of\ control} \times 100$$

ABTS Free Radical Scavenging Method: The ABTS radical scavenging activity of Rs-AgNPs was assessed at various doses using a standardised methodology. A bulk solution of ABTS was generated by combining 7 mM ABTS with 2.45 mM $K_2S_2O_8$, and then incubated at ambient temperature for one day. The stock solution was diluted with ethanol to achieve an absorbance of about 0.85 ± 0.20 at 734 nm, producing the working solution. Subsequently, 20 µL of Rs-AgNPs at different concentrations were introduced into 180 µL of the ABTS working solution. The reaction mixture was incubated at ambient temperature for 30 minutes, followed by absorbance measurement at 734 nm using a Systronic UV-1800 spectrophotometer. Ascorbic acid was utilized as the standard reference, and the ABTS radical scavenging activity was determined using a standard formula.[19]

$$Yield\ \% = \frac{Weight\ of\ extract}{weight\ of\ dried\ plant\ material} \times 100$$

Antidiabetic activity:

Using the α-Amylase and α-Glucosidase assay, Rs-AgNPs were tested for their potential to prevent diabetes.

Inhibition assay of α-amylase:

The test for α-amylase enzyme inhibition was performed with slight changes in the method described by Kaur et al. (2023).[20] Acarbose (AC) functioned as the reference inhibitor for α-amylase. The half-maximal inhibitory concentration (IC_{50}) for each enzyme examined, except α-amylase, was presented as a percentage of inhibition. A particular formula was employed to determine the percentage of inhibition.

$$\%\ of\ Inhibition = \frac{Absorbance\ of\ control\ -\ Absorbance\ of\ extract}{Absorbance\ of\ control} \times 100$$

Inhibition assay of α-glucosidase:

The test for α-glucosidase enzyme inhibition was conducted with little modifications to the methodology described by Kaur et al.[21] Acarbose functioned as the positive control for the inhibition method, with the liberated p-nitrophenol's absorbance being quantified at approximately 400 nm. All experiments were performed in triplicate, except for the test substance. The percentage inhibition for enzymes other than α-glucosidase was evaluated and expressed as IC_{50} values, determined using the aforementioned method.

Antibacterial activity using disc diffusion assay:

The assessment of the antibacterial efficacy of *Raphanus sativus* and the biosynthesized Rs-AgNPs was performed

using the disc diffusion technique. A sterile brush was used to uniformly apply a bacterial inoculum suspension to solidified Muller-Hinton Agar (MHA) plates. The experiment included Gram-positive bacteria, especially *Staphylococcus aureus* (MTCC96) and *Listeria monocytogenes*, as well as Gram-negative bacteria, notably *Escherichia coli* and *Pseudomonas aeruginosa*. Discs were subjected to treatment with Rs-AgNPs at doses of 20, 50, and 75 µg/mL before placement on the infected plates. For 24 hours, the plates were incubated at 37 °C, following which the zones of inhibition were measured in millimetres. Erythromycin (10 µg/disc) functioned as the positive control, whilst DMSO acted as the negative control.[22]

Photocatalytic activity analysis of biosynthesized silver Nanoparticles:

0.1 grams of Ag nanoparticles were disseminated in 100 mL of Methylene Blue (MB) solution, culminating in a concentration of 10 mg/L. The suspension was meticulously agitated in the dark for 30 minutes to guarantee uniformity and attain balance before UV light exposure. At regular intervals, 4 mL of the mixture was withdrawn and centrifuged at 5000 rpm for 10 minutes to separate the Rs-AgNPs from the solution. A Systronics 118 UV-Vis spectrophotometer was used to detect the supernatant absorbance at its peak wavelength of 664 nm.[23,24] The degree of photocatalytic degradation was assessed using the following formula:

Percentage Photodegardation = A_1-AA1×100

A_1 indicates the prior absorbance of the sample, while A signifies the final absorbance of the sample.

Statistical Analysis: The data analysis was conducted using a grouped approach with ANOVA in GraphPad Prism software. When comparing the treatment and control groups, a p-value of less than 0.05 was considered statistically significant. The results are presented as the mean ± standard deviation derived from three independent experiments.

3. Results and discussion

3.1 Extraction and phytochemical analysis

The ethanolic extraction of *Raphanus sativus* leaf material resulted in a yield of 5.26%. The obtained extract was then subjected to qualitative phytochemical screening to identify the bioactive constituents responsible for the reduction and stabilization of AgNPs. The analysis indicated the presence of abundant secondary metabolites (Table 1), which are known to act as reducing agents for silver ions and as capping molecules that prevent nanoparticle aggregation, thereby enhancing their stability. Additionally, polar phytochemicals extracted using polar solvents are recognized for their significant contribution to nanoparticle synthesis and stabilization.[25,26]

Pure extracts derived from leaf components often include a significant diversity of bioactive chemicals, including both primary and secondary metabolites. The predominant components are phenolic compounds such as flavonoids and phenolic acids, which exhibit significant antioxidant and anti-inflammatory properties.[27] Terpenoids and essential oils, especially from aromatic plants, possess antimicrobial and fragrant properties. Saponins and glycosides, including flavonoids and cardiac glycosides, are often present and exhibit antifungal and antiviral properties, as well as immune-modulating effects, respectively. Phytosterols, such as 5-sitosterol, have anti-inflammatory and cholesterol-lowering properties.[28] Proteins, amino acids, carbohydrates, and polysaccharides, essential for nutrition and cellular signalling, may also be extracted from leaves. The content differs across various plant species, extraction solvents, and methodologies used; nonetheless, leaf extracts often include a plethora of multifunctional natural chemicals.[29]

3.2 Characterization details

UV-vis spectroscopy:

The incorporation of *Raphanus sativus* leaf extract into the $AgNO_3$ solution caused a colour transformation from pale yellow to reddish-brown after three hours. This discovery indicates the conversion of Ag^+ to Ag^0 nanoparticles, hence validating the bioformulation of Rs-AgNPs. The UV-vis spectra of the Rs-AgNPs displayed a prominent peak at around 435 nm after 4 hours of incubation. UV-vis spectroscopy is often used for the structural characterisation of nanoparticles.[30,31] The detected absorbance peak at 435 nm is associated with the surface plasmon resonance (SPR) of the AgNPs. Many elements, such as the size and morphology of the nanoparticles, the dielectric properties of the synthesis medium, and the coordination among the nanoparticles, influence the SPR pattern. The augmentation of the SPR band intensity with the time of reaction further corroborates the production of AgNPs (Fig. 1).

Fourier transform infrared spectroscopy:

FTIR spectroscopy was utilised to determine the phytoconstituents present in the decrease and stabilisation of Rs-AgNPs. The FTIR spectra of the Rs-AgNPs exhibited notable absorption peaks at 3343.36, 2915.73, 2853.35, 1590.97, 1301.23, 1015.59, and 815.32 cm^{-1} (Fig. 2), indicating the presence of secondary metabolites acting as capping moieties. The FTIR spectra of the *Raphanus sativus* leaf extract, in conjunction with the Rs-AgNPs, exhibited significant alterations in these peaks, the stabilization, encapsulation, and reduction of the nanoparticles.[32] A shift at 3343.36 cm^{-1} corresponds to O−H or N−H stretching from phenolic chemicals present in the leaf extract. The peak at 2915.73 cm^{-1} signifies C−H stretching linked to methylene oraliphatic groups, characteristic of triterpenoid saponins. Theband at 1590.97 cm^{-1} is due to the stretching of alkenyl or aromatic C=C bonds, while the band at 1301.23 cm^{-1} indicates −C−O stretching often seen in phenols or tertiary alcohols. The peak at 1015.59 cm^{-1} corresponds to O−H stretching in phenolic groups, while the band at 815.32 cm^{-1} is connected with C−O and C−S stretching, often seen in aliphatic chloro compounds.[33,34] The detected peaks are mostly linked to phenolic groups present in alkaloids, polyphenols, terpenes, and saponins, which are abundant in the leaf extract and are

Table 1: Screening of the ethanol extract of *R. sativus* flower for qualitative phytochemical properties.

Phytoconstituents	Ethanol extract
Alkaloids	-
Flavonoids	+
Phenol	+
Saponins	+
Tannins	+
Triterpenoids	+

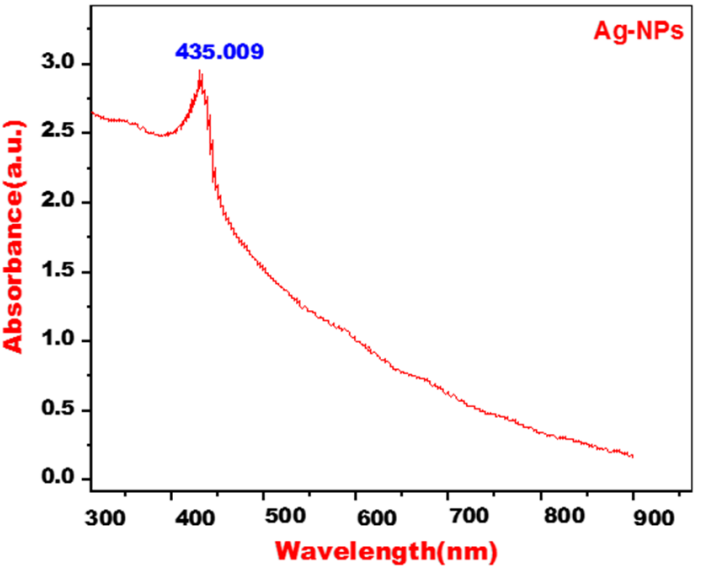

Fig. 1: UV-Vis Absorption spectra of AgNPs.

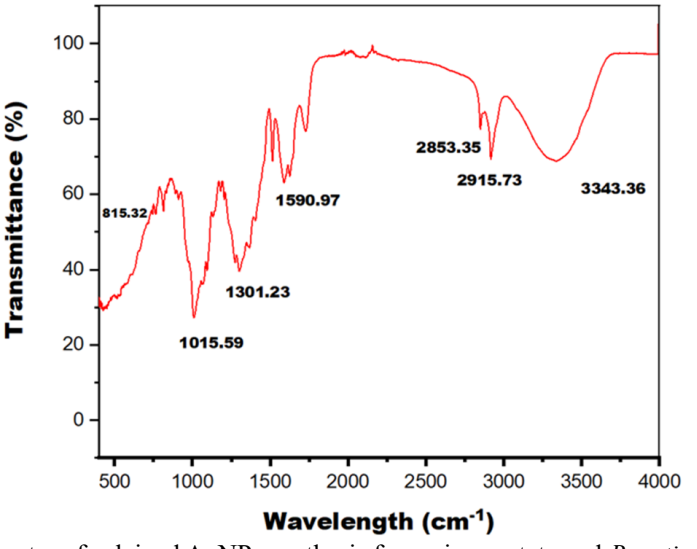

Fig. 2: FTIR spectra of calcined AgNPs synthesis from zinc acetate and *R. sativus* leaf extract.

crucial in the synthesis of Rs-AgNPs. The results are consistent with the phytochemical analysis conducted on *Raphanus sativus* leaves.

Powdered X-ray diffraction:

The Powder X-ray diffraction (PXRD) pattern of the biologically synthesised Rs-AgNPs exhibited unique peaks at 2θ values of 27.45°, 32.35°, 36.84°, 39.15°, 45.78°, 48.53°, 53.78°, and 58.10° (Fig. 3). The observed peaks correspond to the (100), (002), (101), (210), (122), (110), (220), and (311) planes, respectively, validating the face-centered cubic crystal structure, with an average crystallite size of 21.85 nm for the AgNPs. Table 2 summerized miller indices, FWHM values, d-spacing, and average crystallinity of AgNPs. The dimensions of the nanoparticles remarkably affect the patterns seen in XRD peaks. Several reducing agents present in the leaf extract are crucial for stabilising the AgNPs and preserving their crystalline form, a characteristic also seenseen in other biosynthesised nanoparticles.[35]

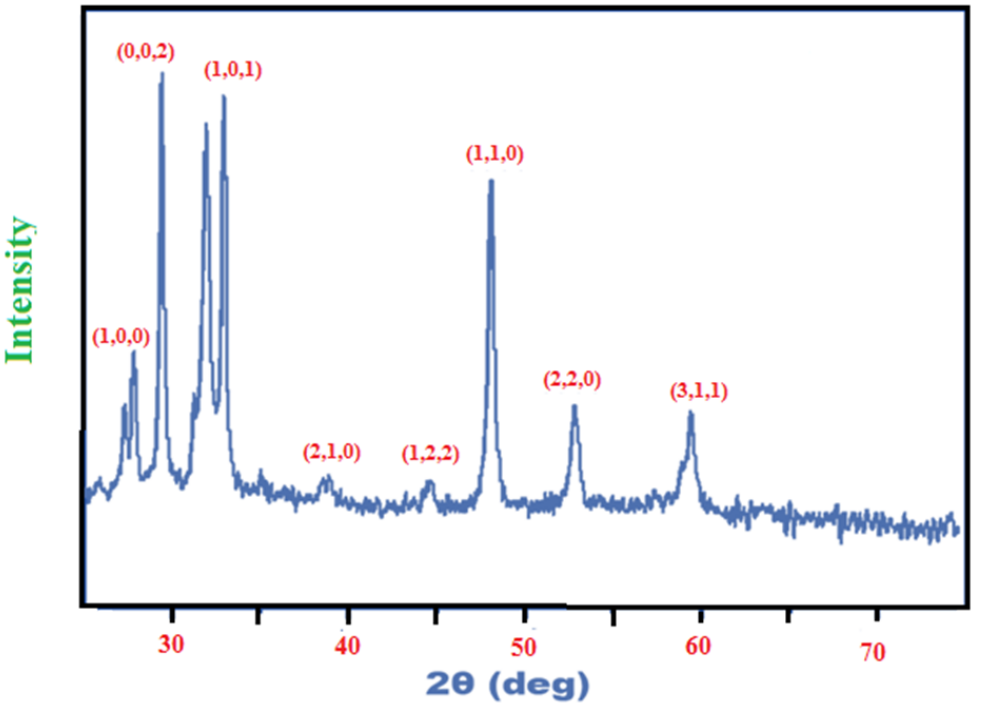

Fig. 3: AgNPs XRD patterns using Silver nitrate and *R. sativus* leaf extract.

Table 2: Miller Indices, FWHM values, d-spacing, and average crystallinity of AgNPs were calculated.

hkl	Pos. [°2Th.]	FWHM Left [°2Th.]	d-spacing [Å]
100	27.4574	0.2453	2.75334
002	30.3578	0.3715	2.83152
101	33.8451	0.3415	2.37877
210	39.1534	0.3154	2.15305
122	45.7855	0.3994	1.98730
110	48.5354	0.3445	1.34558
220	53.7845	0.3671	1.84551
311	58.1045	0.5567	1.23238
Average crystallite size		21.85nm	

The morphology of Rs-AgNPs was analysed using scanning electron microscopy (SEM). The Rs-AgNPs displayed various morphologies, including irregular, granulated, and ellipsoidal shapes, with some observed aggregation (Fig. 4). The SEM investigation indicated that the dimensions of the Rs-AgNPs varied between 30 and 50 nm. The microscopic Investigations indicated that the nanoparticles generally had a spherical morphology and were uniformly dispersed inside the sample. The substantial aggregation of AgNPs may be attributed to the dehydration process that transpired during the sample preparation for SEM examination.[36]

Antioxidant Activity:

The antioxidant efficacy of Rs-AgNPs was assessed *in vitro* using the DPPH and ABTS radical scavenging assays. The results demonstrated a concentration-dependent increase in the inhibition of Rs-AgNPs on both DPPH and ABTS radicals (Fig. 5). Ascorbic acid and quercetin served as positive controls for ABTS and DPPH assays, respectively. Rs-AgNPs exhibited enhanced free radical scavenging activity, with IC_{50} values of **18.41 µg/mL** for DPPH and **25.78 µg/mL** for ABTS, compared to the standard compounds, which recorded IC_{50} values of **9.23 µg/mL** (quercetin for DPPH) and **11.29 µg/mL** (ascorbic acid for ABTS). Although Rs-AgNPs showed slightly lower antioxidant activity than the standards, the results were statistically significant (**$p < 0.05$**) compared to the negative control. The nanoparticles demonstrated effective neutral radical quenching in the DPPH assay and cationic radical scavenging in the ABTS assay. The DPPH test indicated the ability of AgNPs to donate electrons and neutralize free radicals, while the ABTS assay reflected the involvement of both electron and hydrogen atom transfer mechanisms in scavenging cationic free radicals.[37,38]

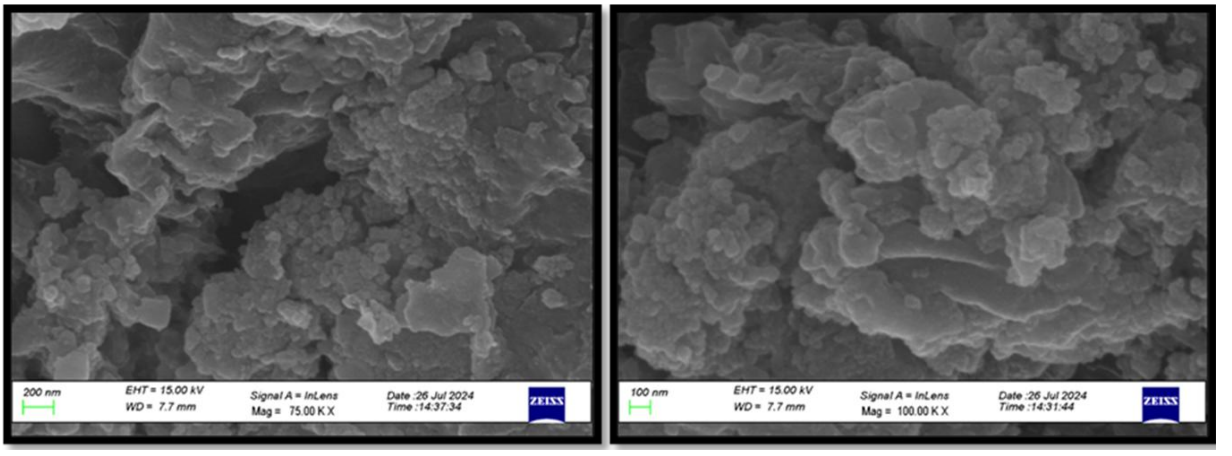

Fig. 4: FESEM images of AgNPs synthesized from ethanolic extract of *R. sativus*.

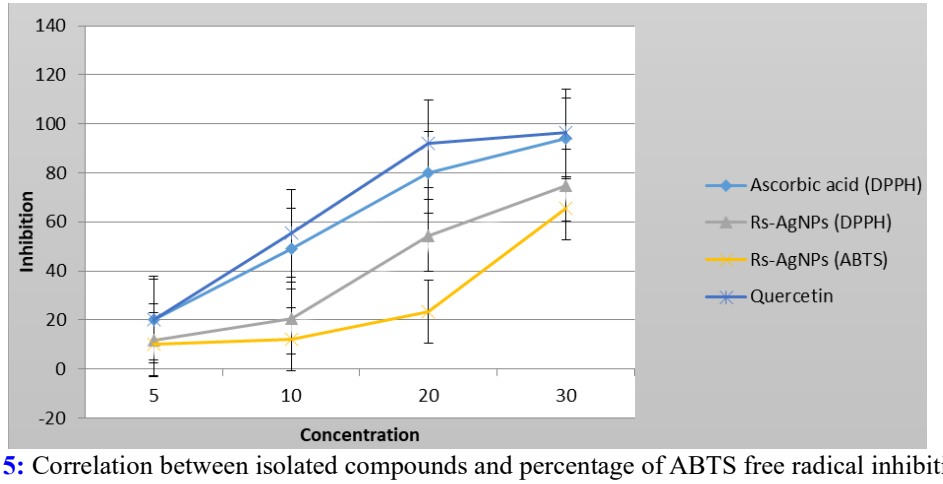

Fig. 5: Correlation between isolated compounds and percentage of ABTS free radical inhibition.

Antidiabetic activity:

Type-2 diabetes mellitus is a prevalent metabolic condition defined by elevated blood glucose levels resulting from inadequate insulin production.[39] Many traditional Indian medicinal herbs have shown effectiveness in diabetes control, providing the benefits of accessibility and few adverse effects. Historically, plants have been a crucial source of medicines, with many modern treatments derived from them.[40] The *in vitro* inhibitory efficacy of Rs-AgNPs on α-amylase was assessed relative to acarbose, as seen in Figure 6. The graph depicts the variation in α-amylase inhibition at different concentrations of Rs-AgNPs, facilitating the determination of the IC_{50} value. The IC_{50} value for Rs-AgNPs was established at **180.34 µg/mL**, indicating substantial α-amylase inhibitory activity. A statistically significant difference was observed when compared to acarbose (**$p < 0.05$**), suggesting the potential of Rs-AgNPs as a natural inhibitor. Similarly, the *in vitro* inhibitory efficacy of Rs-AgNPs on α-glucosidase was evaluated in comparison to acarbose (Fig. 6). The differences in α-glucosidase inhibition at varied sample concentrations enabled the determination of IC_{50} values for both Rs-AgNPs and acarbose. Rs-AgNPs exhibited significant α-glucosidase inhibitory activity, with an IC_{50} value of **150.58 µg/mL**, also showing a statistically significant difference compared to acarbose (**$p < 0.05$**). These results demonstrate that Rs-AgNPs possess promising antidiabetic potential through dual enzyme inhibition.

Antibacterial Activity Using Disc Diffusion Assay:

The assessment of the antibacterial efficacy of Rs-AgNPs was performed by applying the disc diffusion technique, focusing on both Gram-positive bacteria (*S. aureus* and *L. monocytogenes*) and Gram-negative bacteria (*E. coli* and *P. aeruginosa*), as seen in Fig. 7. Rs-AgNPs exhibited significant antibacterial activity, particularly against E. coli and P. aeruginosa, with inhibition zones of 16 mm and 17 mm, respectively, at the highest dose. The antibacterial activity of AgNPs is often more significant in Gram-negative bacteria, perhaps owing to variations in their cell wall composition. Gram-negative bacteria possess one layer of peptidoglycan within their cellular membrane, whereas Gram-positive bacteria have many layers, leading to a more rigid architecture.[32] Silver ions derived from nanoparticles demonstrate a propensity to bind with the negatively charged bacterial cell wall, resulting in modifications to its composition and permeability. This contact obstructs DNA replication and disrupts the expression of ribosomal proteins and other cellular components, resulting in the inactivation of essential enzymes and impeding ATP synthesis.[41,42]

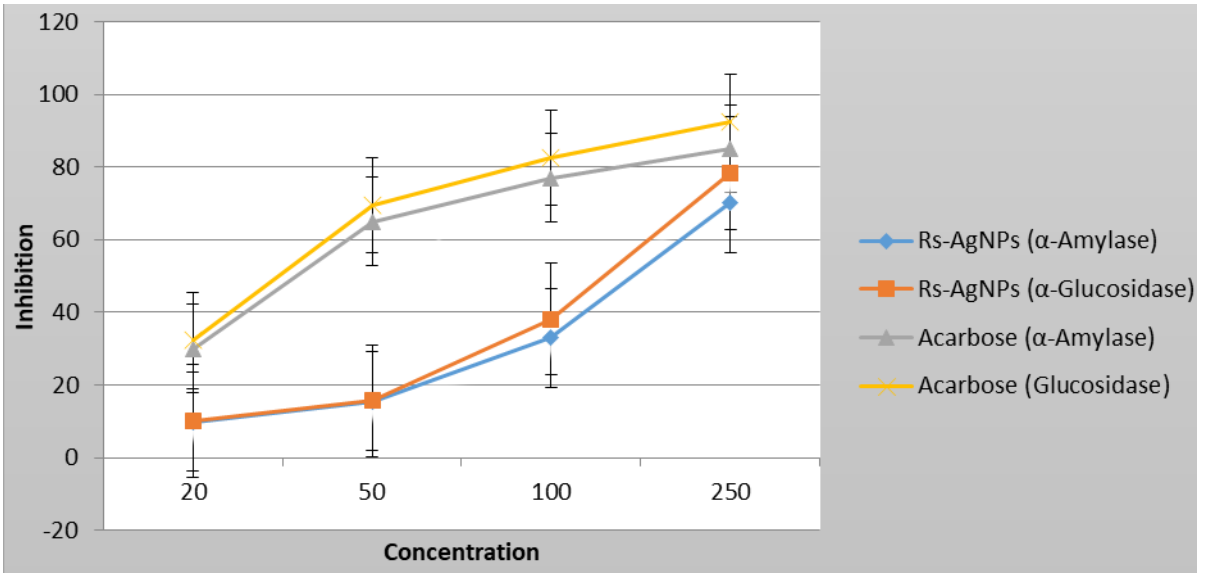

Fig. 6: Correlation between isolated compounds and percentage of α-amylase enzyme inhibition.

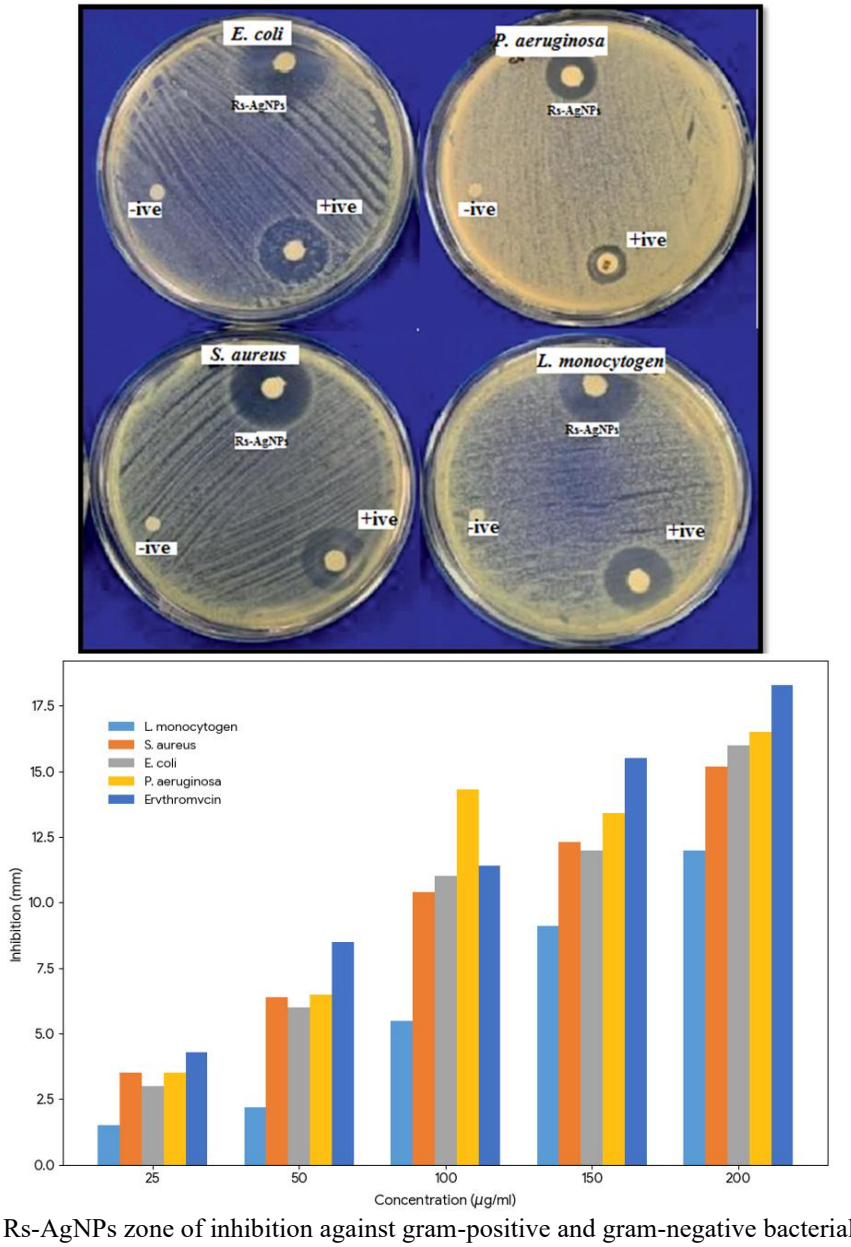

Fig. 7: Rs-AgNPs zone of inhibition against gram-positive and gram-negative bacterial stain.

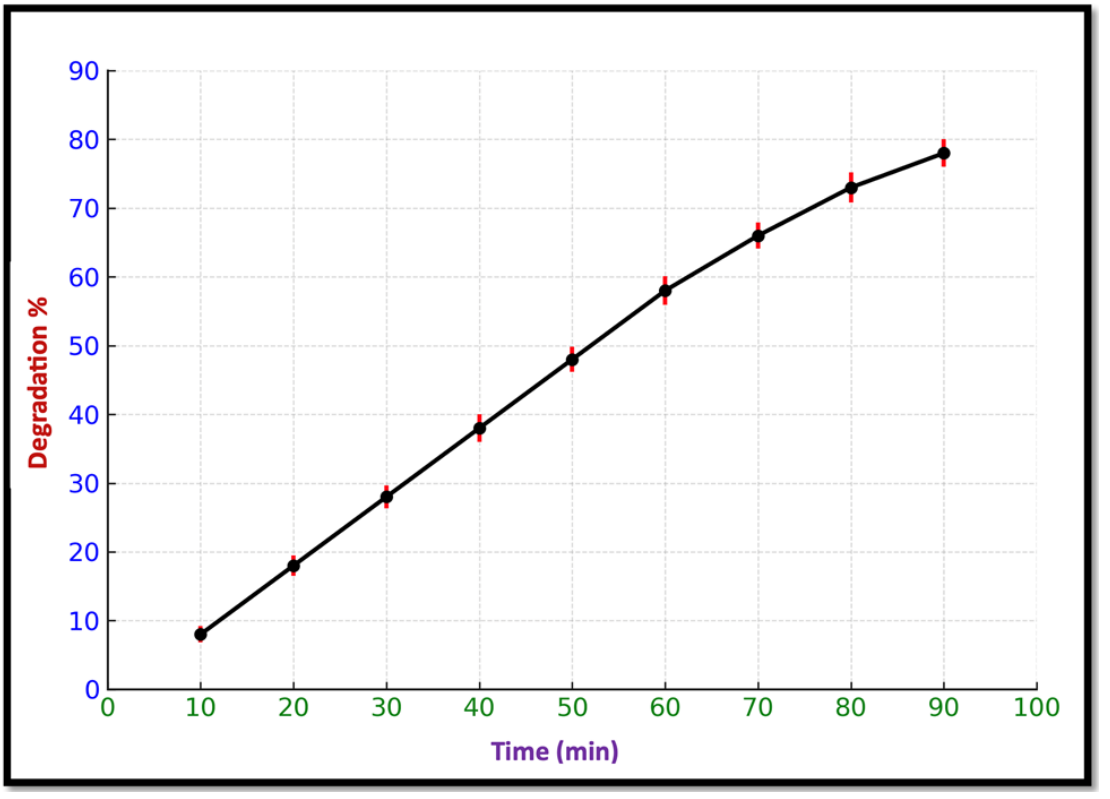

Fig. 8: Percentage degradation of irradiation time vs. methylene blue dye in the presence of the Rs-AgNPs.

Photocatalytic Activity:

The UV light absorption spectrum demonstrated the degradation of MB dye and the role of Rs-AgNPs nanoparticles as photocatalysts, as shown in Figure 8. The decrease in absorbance at 664 nm with time indicates that AgNPs are effectively promoting the degradation process. A degradation efficiency of around 77% was achieved in 90 minutes. The photocatalytic efficacy of the nanoparticles may be elucidated by analysing their surface area, shape, and crystallinity. Enhancing the material's crystallization and area of surface results in improved photocatalytic performance, hence affecting the total degradation efficiency.[43]

An evaluation of the nanoparticles' physicochemical stability under various (environmental) circumstances is not carried out, even though the current work shows that Rs-AgNPs were successfully synthesised and bioactive. Stability is one of the most critical criteria for the practical use of AgNPs. Future systematic investigations on stability will include diverse variables of temperature, pH levels, light exposure, and storage duration.[44] UV-Visible spectroscopy, dynamic light scattering (DLS), and zeta potential analysis will be used to monitor the temporal variations in particle aggregation, surface charge, and size distribution.

4. Conclusion

The biosynthesis of AgNPs using *R. sativus* offers several benefits, including cost-effectiveness, efficiency, and environmental sustainability. This approach enhances energy efficiency, reduces expenses, and promotes healthier workplaces and communities by protecting human health and the environment, resulting in decreased waste and more reliable products. The secondary metabolites responsible for the fabrication of nanoparticles via plant mediation demonstrate biocompatibility, making them suitable for various biomedical applications. Furthermore, the nanoparticles demonstrated photocatalytic, antioxidant, antidiabetic, and antibacterial properties against both Gram-positive and Gram-negative bacteria, with effects that were contingent upon the dosage administered. This investigation highlights another important aspect of *R. sativus*, showcasing its ability to formulate AgNPs with water treatment and medical properties.

Acknowledgments

The authors express their gratitude to the Department of Chemistry at IFTM University, Moradabad, for providing essential facilities, as well as to the Central Laboratory at Delhi University, India.

Conflict of Interest

There is no conflict to declare.

Supporting Information

Not applicable.

CRediT Statement

Sangeeta Gupta: Investigation, Methodology, **Deepanshu Rana, Keshari Nandan:** Resources validation, Visualization, **Amanpreet Kaur, Man Vir Singh:** Original draft, and Writing - Review and editing. **Yogendra Kumar, Shubham**

Sharma, Avnish Chauhan and Santosh Kumar Verma: Conceptualization, Data curation, Formal analysis, Funding acquisition, Investigation, Methodology, Resources, Software, Supervision.

References

[1] L. Song, H. Li, X. Fu, M. Cen, J. Wu, Association of the oxidative balance score and cognitive function and the mediating role of oxidative stress: evidence from the national health and nutrition examination survey (NHANES) 2011–2014, *The Journal of Nutrition*, 2023, **153**, 1974-1983, doi: 10.1016/j.tjnut.2023.05.014.

[2] T. O. Aremu, O. E. Oluwole, K. O. Adeyinka, An understanding of the drivers of infectious diseases in the modern world can aid early control of future pandemics, *Pharmacy*, 2021, **9**, 181, doi: 10.3390/pharmacy9040181.

[3] M. A. Hossain, S. Akhter, M. H. Sohrab, F. Afroz, M. N. Begum, S. Roy Rony, Applying an optimization technique for the extraction of antioxidant components from justicia adhatoda leaves, *Engineered Science*, 2023, **24**, 913, doi: 10.30919/es913.

[4] N. Bashir, A. S. Dablool, M. I. Khan, M. G. Almalki, A. Ahmed, M. Ahmad Mir, A. A. E. Hamdoon, M. A. Elawad, O. F. Mosa, L. N. Niyazov, M. E. M. Elkhalifa, M. A. Alghamdi, A. Anwar, M. Ayaz, Antibiotics resistance as a major public health concern: a pharmaco-epidemiological study to evaluate prevalence and antibiotics susceptibility-resistance pattern of bacterial isolates from multiple teaching hospitals, *Journal of Infection and Public Health*, 2023, **16**, 61-68, doi: 10.1016/j.jiph.2023.09.019.

[5] B. M. Aiesh, M. A. Nazzal, A. I. Abdelhaq, S. A. Abutaha, S. H. Zyoud, A. Sabateen, Impact of an antibiotic stewardship program on antibiotic utilization, bacterial susceptibilities, and cost of antibiotics, *Scientific Reports*, 2023, **13**, 5040, doi: 10.1038/s41598-023-32329-6.

[6] I. N. Z. N. Azmi, S. A. B. M. Taupik, T. S. Chuah, P. W. Chai, Synthesis and phytotoxic test of calcium oxide nanoparticles derived from cassava peels and leaves against selected Malaysian common weeds, *ES Food & Agroforestry*, 2025, **19**, 1410, doi: 10.30919/faf1410.

[7] Z. Mukatayeva, Y. Bakytkarim, W. Nuerbaheti, Y. Tileuberdi, N. Shadin, Z. Assirbayeva, L. Zhussupova, Electrochemical sensor based on silicon carbide and coke-derived carbon nanocomposites for sensitive detection of lead ions, *ES Materials & Manufacturing*, 2025, **29**, 1653, doi: 10.30919/mm1653.

[8] L. Zhu, B. Jing, X. Kou, P. Yuan, Y. Li, L. Li, B. B. Xu, I. Seok, D. Hu, Heteroepitaxial barium titanate/niobium potassium oxide polyimide nanocomposite films for high temperature energy storage, *Engineered Science*, 2025, **36**, 1666, doi: 10.30919/es1666.

[9] S. Aldhanhani, M. Ali, H. Butt, Evolving trends in 3D printing of graphene composites, *ES Materials & Manufacturing*, 2025, **29**, 1682, doi: 10.30919/mm1682.

[10] S. M. El Turk, A. E. Salih, H. Butt, Optimization of *in situ* integration of gold nanoparticles into commercial contact lenses for ophthalmic applications, *ES Materials & Manufacturing*, 2025, 28, 1456, doi: 10.30919/mm1456.

[11] T.-J. Yu, J.-P. Shiau, J.-Y. Tang, A. Ahmad Farooqi, Y.-B. Cheng, M.-F. Hou, C.-H. Yen, H.-W. Chang, Physapruin a exerts endoplasmic reticulum stress to trigger breast cancer cell apoptosis *via* oxidative stress, *International Journal of Molecular Sciences*, 2023, **24**, 8853, doi: 10.3390/ijms24108853.

[12] C. Vairo, M. Villar Vidal, R. Maria Hernandez, M. Igartua, S. Villullas, Colistin- and amikacin-loaded lipid-based drug delivery systems for resistant gram-negative lung and wound bacterial infections, *International Journal of Pharmaceutics*, 2023, **635**, 122739, doi: 10.1016/j.ijpharm.2023.122739.

[13] Y. Liu, R. Zhang, B. Wang, S. Song, F. Zhang, Evaluation of penicillin-resistance and probiotic traits in Lactobacillus plantarum during laboratory evolution, *Gene*, 2024, **891**, 147823, doi: 10.1016/j.gene.2023.147823.

[14] E. Grossini, F. De Marchi, S. Venkatesan, A. Mele, D. Ferrante, L. Mazzini, Effects of acetyl-L-carnitine on oxidative stress in amyotrophic lateral sclerosis patients: evaluation on plasma markers and members of the neurovascular unit, *Antioxidants*, 2023, **12**, 1887, doi: 10.3390/antiox12101887.

[15] A. K. Helmy, N. M. Sidkey, R. E. El-Badawy, A. G. Hegazi, Emergence of microbial infections in some hospitals of Cairo, Egypt: studying their corresponding antimicrobial resistance profiles, *BMC Infectious Diseases*, 2023, **23**, 424, doi: 10.1186/s12879-023-08397-4.

[16] R. G. Roy, P. K. Mandal, J. C. Maroon, Oxidative stress occurs prior to amyloid aβ plaque formation and tau phosphorylation in Alzheimer's disease: role of glutathione and metal ions, *ACS Chemical Neuroscience*, 2023, **14**, 2944-2954, doi: 10.1021/acschemneuro.3c00486.

[17] G. Habibullah, J. Viktorova, T. Ruml, Current strategies for noble metal nanoparticle synthesis, *Nanoscale Research Letters*, 2021, **16**, 47, doi: 10.1186/s11671-021-03480-8.

[18] E. A. Odongo, P. C. Mutai, B. K. Amugune, N. N. Mungai, M. O. Akinyi, J. Kimondo, Evaluation of the antibacterial activity of selected Kenyan medicinal plant extract combinations against clinically important bacteria, *BMC Complementary Medicine and Therapies*, 2023, **23**, 100, doi: 10.1186/s12906-023-03939-4.

[19] K. Mohlala, U. Offor, E. Monageng, N. B. Takalani, C. S. Opuwari, Overview of the effects of moringa oleifera leaf extract on oxidative stress and male infertility: a review, *Applied Sciences*, 2023, **13**, 4387, doi: 10.3390/app13074387.

[20] J. Tchekalarova, R. Tzoneva, Oxidative stress and aging as risk factors for Alzheimer's disease and Parkinson's disease: the role of the antioxidant melatonin, *International Journal of Molecular Sciences*, 2023, **24**, 3022, doi: 10.3390/ijms24033022.

[21] H. Vergara-Castañeda, L. O. Granados-Segura, G. Luna-Bárcenas, D. J. McClements, M. G. Herrera-Hernández, N. Arjona, A. R. Hernández-Martínez, M. Estevez, H. Pool, Gold nanoparticles bioreduced by natural extracts of arantho (*Kalanchoe daigremontiana*) for biological purposes: physicochemical, antioxidant and antiproliferative evaluations, *Materials Research Express*, 2019, **6**, 055010, doi: 10.1088/2053-1591/ab0155.

[22] A. Kaur, M. V. Singh, N. Bhatt, S. Arora, A. Shukla,

Exploration of chemical composition and biological activities of the essential oil from ehretia acuminata R. Br. fruit, *ES Food & Agroforestry*, 2023, **15**, 1068, doi: 10.30919/esfaf1068.
[23] A. Kaur, A. Shukla, R.K. Shukla, In vitro antidiabetic and anti-inflammatory activities of the bark of Ehretia acuminata R. Br, *Indian Journal of Natural Products and Resources*, 2022, **12**, 538-43, doi: 10.56042/ijnpr.v12i4.29108.
[24] C. Cruz Paredes, P. Bolívar Balbás, A. Gómez-Velasco, Z. N. Juárez, E. Sánchez Arreola, L. R. Hernández, H. Bach, Antimicrobial, antiparasitic, anti-inflammatory, and cytotoxic activities of *Lopezia racemosa*, *The Scientific World Journal*, 2013, **2013**, 237438, doi: 10.1155/2013/237438.
[25] B. Zamani, F. Taghvaee, H. Akbari, A. Mohtashamian, N. Sharifi, Effects of selenium supplementation on the indices of disease activity, inflammation and oxidative stress in patients with rheumatoid arthritis: a randomized clinical trial, *Biological Trace Element Research*, 2024, **202**, 1457-1467, doi: 10.1007/s12011-023-03782-1.
[26] N. Bhatt, M. S. Mehata, A sustainable approach to develop gold nanoparticles with kalanchoe fedtschenkoi and their interaction with protein and dye: sensing and catalytic probe, *Plasmonics*, 2023, **18**, 845-858, doi: 10.1007/s11468-023-01814-z.
[27] S. Gupta, M. V. Singh, M. Rani, S. Arora, S. D. Sharma, A. Kaur, Transforming fruit and vegetable waste into nanoparticles: a step towards sustainable nanotechnology, *Natural Product Communications*, 2025, **20**, 1934578X251346010, doi: 10.1177/1934578x251346010.
[28] H. D. Beyene, A. A. Werkneh, H. K. Bezabh, T. G. Ambaye, Synthesis paradigm and applications of silver nanoparticles (AgNPs), a review, *Sustainable Materials and Technologies*, 2017, **13**, 18-23, doi: 10.1016/j.susmat.2017.08.001.
[29] J. L. Mejía-Méndez, H. Bach, A. C. Lorenzo-Leal, D. E. Navarro-López, E. R. López-Mena, L. R. Hernández, E. Sánchez-Arreola, Biological activities and chemical profiles of kalanchoe fedtschenkoi extracts, *Plants*, 2023, **12**, 1943, doi: 10.3390/plants12101943.
[30] L. I. Bazylyak, A. R. Kytsya, P. Y. Lyutyy, N. I. Korets'ka, Y. V. Pilyuk, O. I. Kuntyi, Silver nanoparticles produced *via* a green synthesis using the rhamnolipid as a reducing agent and stabilizer, *Applied Nanoscience*, 2023, **13**, 5251-5263, doi: 10.1007/s13204-022-02751-9.
[31] K. D. Dejen, D. Y. Kibret, T. H. Mengesha, E. T. Bekele, A. Tedla, T. A. Bafa, F. T. Derib, Green synthesis and characterisation of silver nanoparticles from leaf and bark extract of*Croton macrostachyus*for antibacterial activity, *Materials Technology*, 2023, **38**, 2164647, doi: 10.1080/10667857.2022.2164647.
[32] P. B. Dahivade, S. N. Pawar, H. M. Pathan, B. J. Lokhande, Temperature-dependent hydrothermal synthesis of CdO nanoparticles and its analysis for supercapacitor application, *ES Energy & Environment*, 2024, **24**, 1098, doi: 10.30919/esee1098.
[33] M. Danaei, M. Dehghankhold, S. Ataei, F. Hasanzadeh Davarani, R. Javanmard, A. Dokhani, S. Khorasani, M. R. Mozafari, Impact of particle size and polydispersity index on the clinical applications of lipidic nanocarrier systems, *Pharmaceutics*, 2018, **10**, 57, doi: 10.3390/pharmaceutics10020057.
[34] R. Verma, A. B. Khan, A. K. Amar, M. I. K. Khan, S. Sah, Opto-structural characteristics and biomedical applications of microwave irradiated green synthesised AM-agnp from atalantia monophylla (L.) leaf extract, *ES Energy & Environment*, 2022, **17**, 44-55, DOI: 10.30919/esee8c745.
[35] A. Kaur, M. V. Singh, A. Shukla, M. Sethi, P. Jayaswal, P. Singhal, E. Kyrbassova, N. Altybayeva, S. Sharma, G. Baigaziyeva, Isolation, characterization and utilization of secondary metabolites from ehretia acuminata: involve exploring bioactive compounds for pharmaceutical and industrial applications, *ES Food & Agroforestry*, 2025, **20**, 1447, doi: 10.30919/faf1447.
[36], M. Khater, G. Kulkarni, S. Khater, *In vitro* evaluation of TiO_2 nanoparticles for enhanced antibacterial and cytotoxicity activities, *ES Materials & Manufacturing*, 2024, **26**, 1266, doi: 10.30919/esmm1266.
[37] Q. U. Ain, M. Alkadi, J. Munir, S. M. H. Qaid, A. A. Ali Ahmed, Green synthesis of silver nano particles using *Dracaena Trifasciata* plant extract and comparison of fatty acids and amides capping agents, *Physica Scripta*, 2023, **98**, 125969, doi: 10.1088/1402-4896/ad0882.
[38] S. Shafique, S. Arif, U. Batool, I. Ahmed, G. A. Khan, R. Shahbaz, M. Imran, H. Butt, J.-F. Masson, D. de Chimie Institut Courtois Centre Québécois des Matériaux Fonctionnels CQMF and Regroupement Québécois des Matériaux de Pointe RQMP Université de Montréal C. P. Succ. Centre-Ville Montréal QC HC J Canada, W. Ahmed, Facile fabrication of hollow silver-gold alloy nanostructures directly on filter paper for enhanced catalytic and antibacterial applications, *ES Materials & Manufacturing*, 2025, **28**, 1505, doi: 10.30919/mm1505.
[39] G. A. Molina, R. Esparza, J. L. López-Miranda, A. R. Hernández-Martínez, B. L. España-Sánchez, E. A. Elizalde-Peña, M. Estevez, Green synthesis of Ag nanoflowers using Kalanchoe Daigremontiana extract for enhanced photocatalytic and antibacterial activities, *Colloids and Surfaces B: Biointerfaces*, 2019, **180**, 141-149, doi: 10.1016/j.colsurfb.2019.04.044.
[40] A. Kayumova, P. Zhanbirbayeva, A. Kuanyshbekova, A. Baltabekov, N. Ibrayev, Z. Idrisheva, T. Serikov, Effect of silver concentration on the photocatalytic activity of a nanocomposite based on titanium dioxide nanorods and reduced graphene oxide, *Engineered Science*, 2025, **38**, 1890, doi: 10.30919/es1890.
[41] M. Zhaisanbayeva, G. S. Patrin, K. Seitbekova, M. Nurbekova, M. Mataev, Synthesis and structural studies of perovskite-ytterbium manganate and spinel-cobalt chromite nanomaterials, *Engineered Science*, 2025, **34**, 1469, doi: 10.30919/es1469.
[42] S. Matarneh, N. Louzi, I. Asi, M. Abdel-Jaber, E. Masad, Genetic expression programming (GEP) based empirical models for the prediction of rutting parameter of bitumen modified using nanomaterials, *Engineered Science*, 2025, **34**, 1438, doi: 10.30919/es1438.
[43] S. Aldhanhani, M. Ali, R. A. Elkaffas, H. Butt, Y. A. Samad,

Advancing structural integrity: graphene nanocomposites *via* vat photopolymerization 3D printing, *ES Materials & Manufacturing*, 2024, **26**, 1303, doi: 10.30919/esmm1303.
[44] S. Jalgar, A. M. Hunashyal, B. S. Maddodi, Damping ratio measurement through modal analysis of smart hybrid nanocomposite internal damper to absorb critical energy in concrete structures, *ES Materials & Manufacturing*, 2025, **27**, 1443, doi: 10.30919/mm1443.